

# Novel Folate-Hydroxamate Based Antimetabolites: Synthesis and Biological Evaluation

Marta P. Carrasco<sup>a</sup>, Eva A. Enyedy<sup>a</sup>, Natalia I. Krupenko<sup>b</sup>, Sergey A. Krupenko<sup>b</sup>, Elisa Nuti<sup>c</sup>, Tiziano Tuccinardi<sup>c</sup>, Salvatore Santamaria<sup>c</sup>, Armando Rossello<sup>c</sup>, Adriano Martinelli<sup>c</sup> and M. Amélia Santos<sup>a\*</sup>

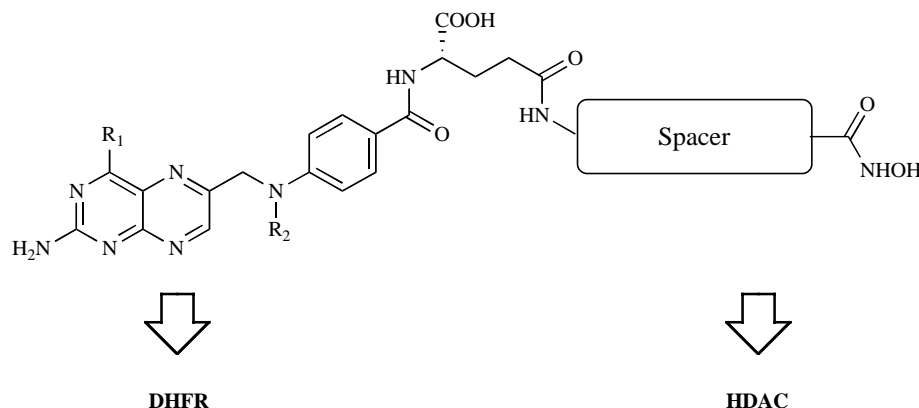
<sup>a</sup>Centro de Química Estrutural, Instituto Superior Técnico, 1049-001 Lisboa, Portugal

<sup>b</sup>Department of Biochemistry and Molecular Biology, Medical University of South Carolina, Charleston, SC, 29425, USA

<sup>c</sup>Dipartimento di Scienze Farmaceutiche, Università di Pisa, Via Bonanno 6, 56126, Pisa, Italy

**Abstract:** A set of hydroxamate derivatives of folic acid and methotrexate (MTX) was synthesized and evaluated for the inhibitory activity against histone deacetylase (HDAC) and dihydrofolate reductase (DHFR), two enzymes overexpressed in metastasizing tumors. The synthesized compounds were further screened for their antiproliferative activity in two human cancer cell lines, A549 (non-small cell lung carcinoma) and PC-3 (prostate adenocarcinoma). All derivatives showed significant inhibitory activity against HDACs (micromolar range) while only the MTX derivative was reasonably effective in DHFR inhibition. A docking study provided insight into the binding mode of the most potent inhibitor in the active sites of the enzymes, allowing rationalization of the bioassays. The MTX-based compound could be of interest for testing against metastasizing tumors in an animal model. The studied derivatives represent promising molecular templates for further development of dual activity anti-cancer drugs.

## Graphical Abstract:



**Keywords:** Antiproliferative, cancer therapy, dihydrofolate reductase inhibitors, dual enzyme inhibitors, folates and antifolates, histone deacetylase inhibitors, methotrexate.

## INTRODUCTION

One of the promising recent strategies for cancer therapy is based on the generation of compounds affecting multiple, sometimes unrelated, cancer cell targets [1-3]. Methotrexate (MTX), one of the oldest anticancer drugs in clinical use [4], is an attractive candidate to be used as a carrier for the second chemical pharmacophore in this hybrid drug approach. Although MTX is a structural analogue of folic acid, it be-

longs to a class of drugs known as antifolates. It inhibits dihydrofolate reductase (DHFR), a key enzyme in folate metabolism [5,6], by binding strongly to the hydrophobic folate-binding pocket of the enzyme [7]. The downstream mechanism, associated with targeting of DHFR by MTX, is the inhibition of the *de novo* synthesis of dTMP and purine nucleotides with ultimate blockage of DNA biosynthesis. This further results in the accumulation of DNA damage and cytotoxicity [7,8]. Of note, MTX has been successfully used in combination with other drugs for treatment of cancer [5].

Another class of rapidly emerging chemotherapeutic agents is histone deacetylase (HDAC) inhibitors (HDACIs) [9]. HDACs are important regulators of chromatin remodel-

\*Address correspondence to this author at the Centro de Química Estrutural, Instituto Superior Técnico, 1049-001 Lisboa, Portugal; Tel: +351 21 841 92 73; Fax: +351 21 846 44 55; E-mail: masantos@ist.utl.pt

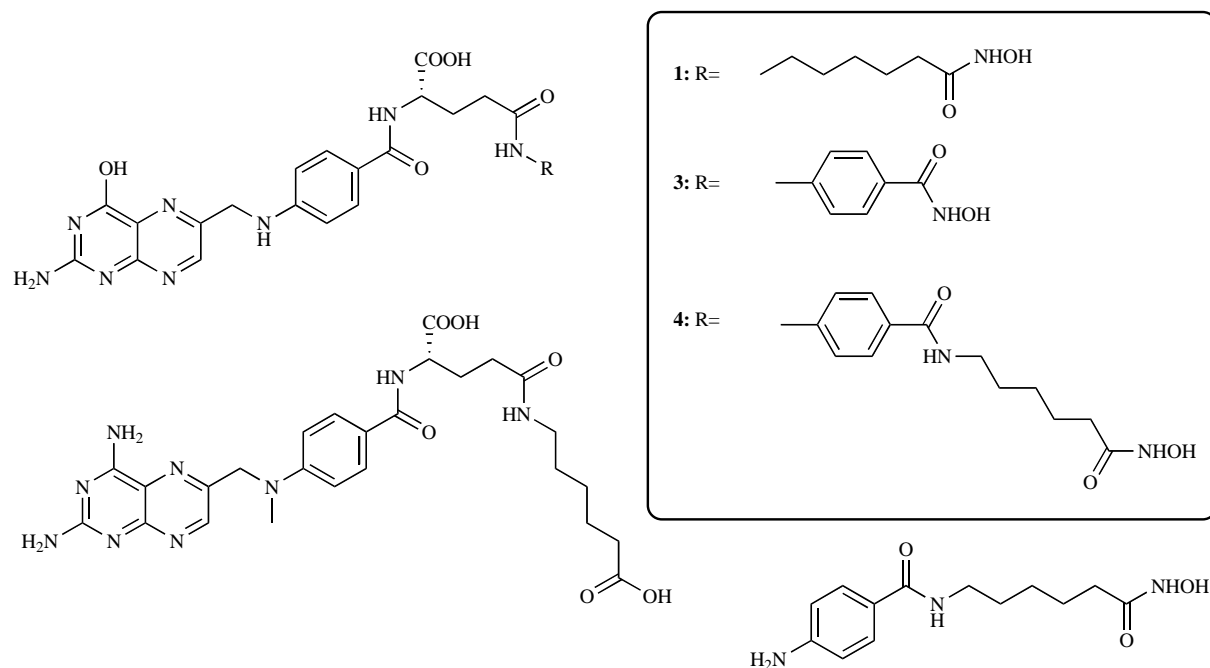


**Fig. (1).** Structures of the synthesized compounds.

ing and their inhibition drastically alters gene expression and induces apoptosis in tumor cells [10]. In addition to histones, HDACs target other acetylated proteins, including a variety of transcription factors [11]. Therefore, the antiproliferative effects of HDACIs likely involve multiple mechanisms. The inhibitors can change the expression of 7-10% of genes and induce differentiation, cell-cycle arrest, and apoptosis in transformed cell cultures [12,13]. In October 2006, the US FDA approved one such inhibitor, SAHA, for the treatment of cutaneous T-cell lymphoma [14], and several new inhibitors are in different phases of clinical trials at present [9].

The recent paradigm of multifunctional pharmacology emerged as a rather efficient way to treat complex diseases, such as cancer. It involves the use of either multiple drugs directed toward multiple targets or the use of a single compound with multiple activities [15]. Recent studies reported the use of HDACIs in combination with other anticancer drugs, namely with 5-fluorouracil, an antimetabolite used to treat breast and colorectal cancers [16]. The enhanced efficacy of these inhibitor combinations suggests very promising future therapeutic applications of HDACIs [17-19].

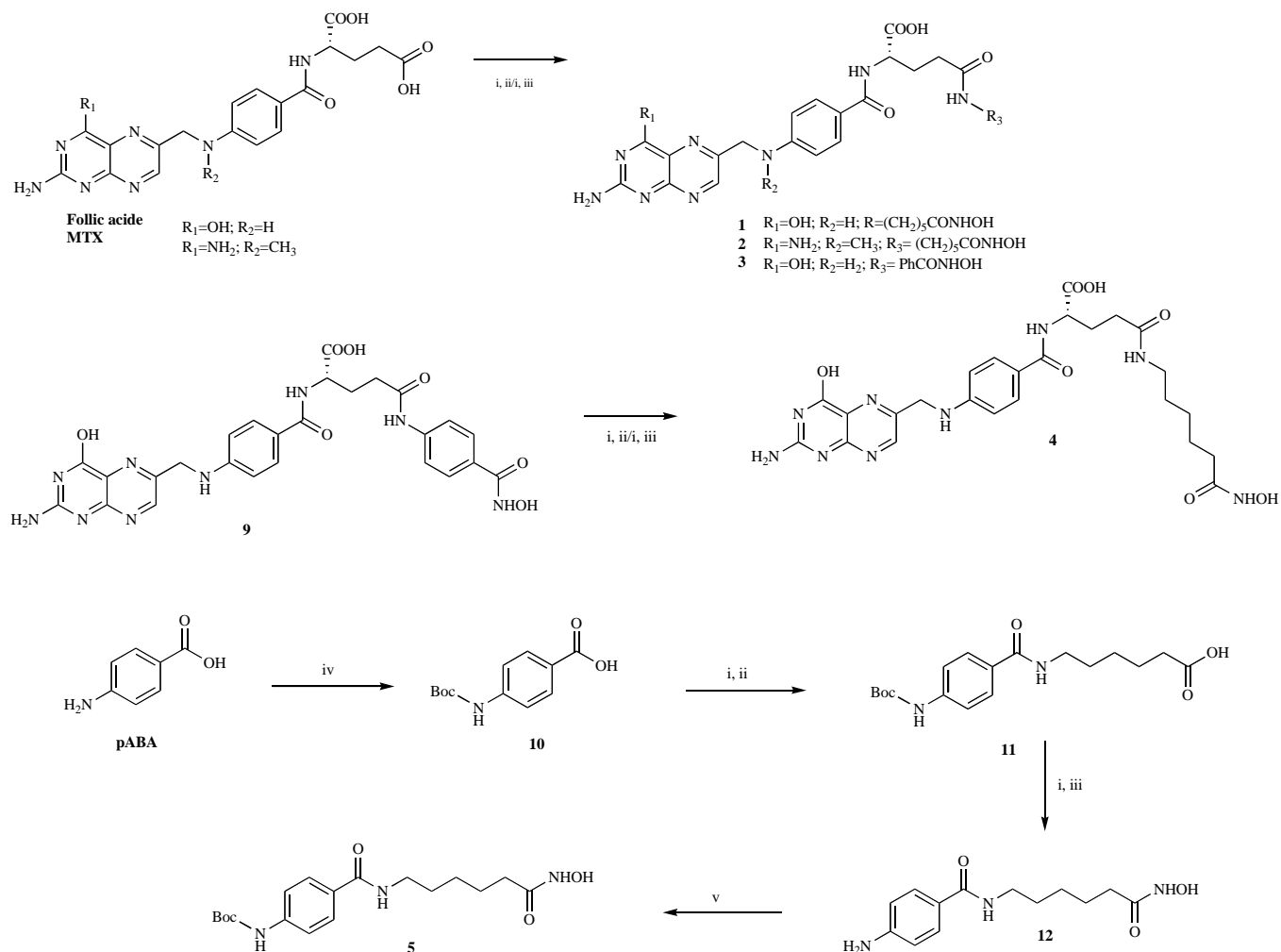
Following our recent research interest in the development of multifunctional compounds for the treatment of complex multifactorial diseases [20], in particular, the use of antifolates bearing an additional functional group [21,22], we have developed a series of hybrid compounds for simultaneous inhibition of DHFR and HDACs, two important targets in drug development for the treatment of several diseases. These compounds are based on the combination of two main functional groups, MTX/folate and hydroxamate which are connected by different spacers to allow for optimization of the ligand-enzyme interactions. Herein we describe the design and synthesis of the compounds and their inhibitory activities against DHFR and HDAC8, and their anti-proliferative effects on two human cancer cell lines, A549 and PC3. We also employed a molecular docking approach

to gain insight into the molecular interactions responsible for the observed biological effects.

## RESULTS AND DISCUSSION

### Molecular Design

The strategy for the design of the dual-targeting compounds is based on a combination, in a single molecule, of the two active functional groups capable of targeting and inhibiting two different enzymes. Specifically, the newly synthesized compounds include the aminopteridine nucleus, to enable the DHFR inhibition, and a primary hydroxamate moiety, as the zinc-binding group (ZBG), to inhibit HDAC via coordination to its zinc-cofactor. The two moieties are connected through long flexible spacers (similarly to SAHA) to enable the ZBG access to the zinc ion bound in the HDAC active site (this ion is situated on the bottom of a long narrow channel in the protein molecule). To preserve the structural determinants of MTX, essential for the binding with DHFR, the molecule was modified by attaching the aminocaproic hydroxamic acid to the  $\gamma$ -carboxylic group of the glutamate. The corresponding folic acid derivatives were also synthesized and studied. The rationale for studying these derivatives was a potential for increased delivery of hydroxamate due to the elevated levels of folate receptor in cancer cells [23]. Since the potency of the HDAC inhibitors depends on their accommodation at the active site of the enzyme, the folic acid derivatives were designed with different spacer groups between the core molecule and the hydroxamate ZBG, namely through variation of the chain length and insertion of phenyl group *para*-aminobenzoic acid (*pABA*)-caproic hydroxamic acid was also synthesized as the simple analogue model, containing only one of the two functional groups. Overall, the following derivatives of MTX and folic acid were synthesized and tested (Fig. 1): folate-caproic hydroxamic acid (1), methotrexate-caproic hydroxamic acid



**Scheme 1.** Synthesis of the  $\gamma$ -hydroxamic acid derivatives of MTX and folic acid and *p*ABA-caproic hydroxamic acid. Reagents and conditions: (i) TBTU, NMM, 0 °C, dry DMF; (ii) amino acid (6-amino-caproic acid, *p*ABA), 0 °C, dry DMF; (iii)  $NH_2OH$ , 0 °C, dry DMF; (iv)  $Na_2CO_3$ ,  $Boc_2O$ , 0 °C, water, 1,4-dioxane; (v) TFA,  $CH_2Cl_2$ , RT.

(2), folate-*p*ABA hydroxamic acid (3), folate-*p*ABA-caproic hydroxamic acid (4) and *p*ABA-caproic hydroxamic acid (5).

### Chemistry

The methotrexate derivative 2 and the folic acid derivatives 1, 3, and 4 were synthesized as described in Scheme 1.

The first step of the synthetic process involved the coupling of an amino group of amino acid molecules (6-amino-caproic acid or *p*ABA) to the  $\gamma$ -carboxylic group of folic acid or MTX, with the preceding carboxylic group activation by stoichiometric amount of TBTU in the presence of *N*-methyl-morpholine (NMM). The rationale for this carboxylic activation (use of a bulky activating group and strict equivalent amount of folate/MTX and TBTU) was the promotion of the coupling of the amine group to the  $\gamma$ -carboxylic group due to hindrance of the  $\alpha$ -position by the bulky activating agent. For the precursor of folate-*p*ABA-caproic hydroxamic acid (5), the 6-amino-caproic acid was coupled to the activated folate-*p*ABA acid. The last step was always the conversion of the terminal carboxylic group of the new amino acid derivative to the corresponding hydroxamic acid analogue through condensation with the free hydroxylamine.

This last step involves, once more, the use of TBTU as the activating agent.

With regard to *p*ABA-caproic hydroxamic acid (5), the preparation of the corresponding precursor, *p*ABA-caproic acid, involved an initial protection of the *p*ABA amino group with Boc, with standard deprotection using TFA as the last step.

### HDACs Inhibition

The synthesized derivatives and the reference compound Trichostatin A (TSA) were tested for HDAC inhibition. Recombinant human HDAC8 or crude nuclear extract from HeLa cells were used as target enzymes in fluorimetric assays (Table 1). HDAC8 isoform was selected for the assays since its X-ray crystal structure is currently available. This enabled us to correlate the inhibitory activity and the interactions between the inhibitors and targeted active sites.

With regard to HDAC8 inhibition, among all derivatives, the model *p*ABA-caproic hydroxamic acid (5) showed quite good inhibitory activity with  $IC_{50}$  value in a micromolar range, lower than those for the aminocaproic acid derivatives of folate or MTX. Folate-caproic hydroxamic acid (1) and

**Table 1. Inhibitory Activities of the  $\gamma$ -hydroxamic Acid Derivatives of MTX and Folate and of the *p*ABA-caproic Hydroxamic Acid, as well as the Reference Drug (TSA) Against Human HDAC8 and the HDACs of the Crude Nuclear Extract from HeLa Cells (IC<sub>50</sub>,  $\mu$ M)**

Compound	Human HDAC8	HeLa Nuclear Extract
folate-caproic hydroxamic acid (1)	23 $\pm$ 4	5.5 $\pm$ 0.3
methotrexate-caproic hydroxamic acid (2)	29 $\pm$ 5	5.7 $\pm$ 0.2
folate- <i>p</i> ABA hydroxamic acid (3)	10.8 $\pm$ 1	1.9 $\pm$ 0.1
folate- <i>p</i> ABA-caproic hydroxamic acid (4)	6.6 $\pm$ 0.8	0.88 $\pm$ 0.08
<i>p</i> ABA-caproic hydroxamic acid (5)	13 $\pm$ 1.7	0.34 $\pm$ 0.01
TSA	1	0.005

methotrexate-caproic hydroxamic acid (2) demonstrated similar inhibitory activities, due to obvious structural similarities. Probably only minor differences in additional secondary interactions within the HDAC catalytic site took place. Changing the linker chain from the amino-caproic acid (compound 1) to the *p*ABA (compound 3) leads to an increased inhibitory activity (IC<sub>50</sub> decreased from 23 to 10.8  $\mu$ M). The most active compound of this series was 4 (IC<sub>50</sub> = 6.6  $\mu$ M), the one with the longest linker chain (a conjugation of *p*ABA with amino-caproic acid). These results suggest correlation between the spacer length and the inhibitory effect. Apparently, this phenomenon may be associated with greater accessibility of the HDAC-bound zinc to the hydroxamate more remotely positioned from the bulky pteridine core. Similarly, introduction of such a linker into MTX derivative might increase the interactions with the active site of HDAC, and improve the inhibitor's activity.

All compounds were also tested for their inhibitory activity against a mix of HDACs, using the crude nuclear extract from HeLa cells (human cervical cancer cell line) as the source of HDACs (Table 1). This assay provided IC<sub>50</sub> values 5-fold lower than those obtained for isolated HDAC8. Compound 4 was still the most active folate derivative, with IC<sub>50</sub> of 0.88  $\mu$ M. Surprisingly, compound 5 showed a higher activity against mixed HDACs (IC<sub>50</sub> = 0.34  $\mu$ M). The reference compound TSA was also more active in this assay than with HDAC8.

### DHFR Inhibition

Inhibitory activities of the synthesized MTX and folic acid derivatives against DHFR are summarized in Table 2. Purified *L. casei* DHFR was used for evaluation of inhibitory activities of the compounds. *L. casei* enzyme proved to be a satisfactory model for such experiments previously [24]. With no surprise, our experiments revealed that the MTX derivative 2 displayed the strongest activity toward DHFR with the IC<sub>50</sub> value in a hundreds nanomolar range. In contrast, the folate analogs showed weak inhibition (high micromolar range). Compared to MTX, however, the hydroxamate derivative of MTX displayed considerably lower DHFR inhibitory activity.

### Cell Proliferation Studies

The antiproliferative activities of the hydroxamate derivatives of folate and MTX were evaluated on A549 (non-

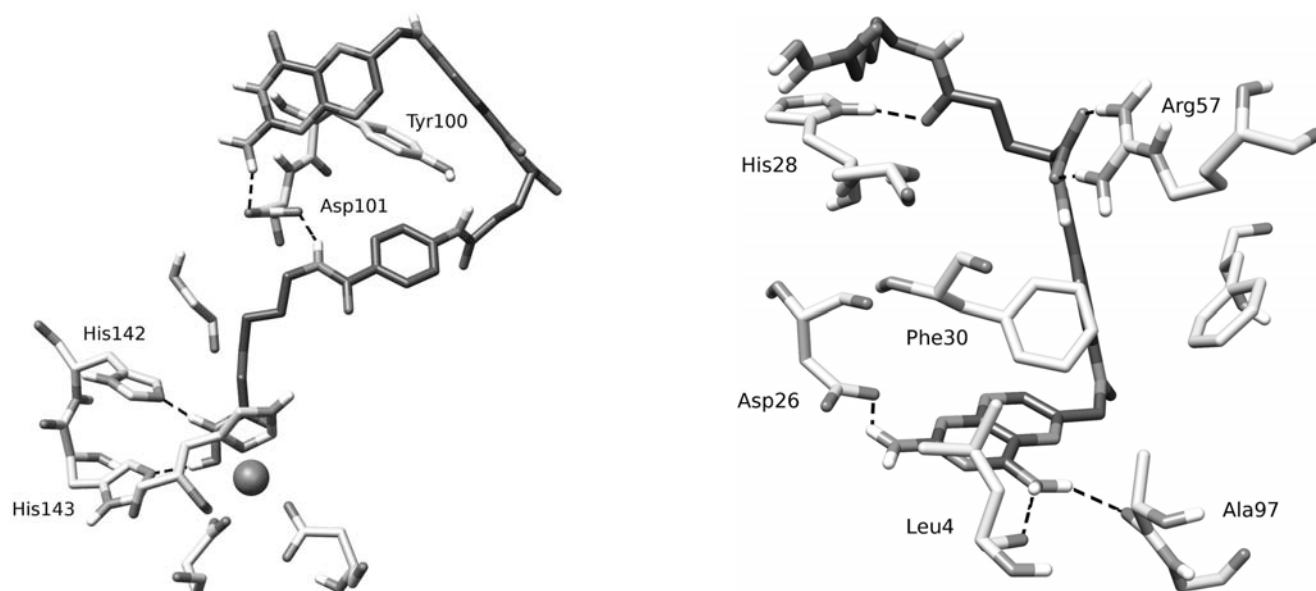
small cell lung carcinoma) and PC-3 (human prostate cancer) cells (Table 2). The model compound 5 presented a low IC<sub>50</sub> value, which could not be rationalized by the direct interaction with the active site of DHFR, but rather by the effect on other important enzymes overexpressed in cancer cells, namely HDAC (due to the demonstrated above high inhibitory activity of this compound against the enzyme). Among the synthesized compounds, the MTX derivative presented much stronger anti-proliferative activity than the folate derivatives. Nevertheless, its activity was considerably weaker than that of MTX itself, which could be explained by the lack of intracellular polyglutamylation due to replacement of the MTX  $\gamma$ -carboxylic group by the hydroxamate moiety. Since folic acid is not a DHFR inhibitor, but one of its substrates, and it is not toxic even at high concentrations, the lack of activity for the folic acid derivatives was somewhat anticipated. The folic acid moiety was expected to enhance the transport of the attached hydroxamate into the cells, increase the effective concentration of HDACI and suppress proliferation through folate-independent pathways. Apparently, this was not the case in our experiments: IC<sub>50</sub> for these compounds in both cell lines were over 100 times higher than their respective IC<sub>50</sub> towards the HeLa nuclear HDACs. Also, none of the tested inhibitors was as effective as MTX itself (IC<sub>50</sub> for MTX is 1 nM, while for all derivatives it is in medium-high micromolar range). In general, among the studied compounds, the MTX hydroxamate demonstrated the best inhibitory activity against DHFR (micromolar range). This finding suggests that the growth suppressor effects resulted from DHFR inhibition and these should be attributed to the MTX component.

### Docking Studies

To gain an idea of the structural basis for the observed inhibitory effects we have evaluated the binding characteristics of the active molecules using docking studies of folate-*p*ABA-caproic hydroxamic acid (4) and methotrexate-caproic hydroxamic acid (2), in the active site of HDAC8 and DHFR, respectively. The program, GOLD, was used for docking calculations after an extensive conformational search using the available scoring functions (GoldScore, ChemScore and ASP). Application of the GoldScore function by the GOLD program allowed successful prediction of the arrangements of the ligands co-crystallized in the respective enzyme active site: SAHA for HDAC8 and MTX in the

**Table 2. Inhibitory Activities of the Synthesized Compounds and Reference Drug MTX Against *L. casei* DHFR and Antiproliferative Effect on Cancer Cell Lines (IC<sub>50</sub>,  $\mu$ M)**

Compound	<i>L. casei</i> DHFR	Antiproliferative Activities								
		A594 Cells ( $\times 10$ )	PC-3 Cells ( $\times 10$ )							
folate-caproic hydroxamic acid (1)	60	45	70							
methotrexate-caproic hydroxamic acid (2)	0.25	5	6							
folate- <i>p</i> ABA hydroxamic acid (3)	360	46	70							
folate- <i>p</i> ABA-caproic hydroxamic acid (4)	20	70	<i>p</i> ABA-caproic hydroxamic acid (5)	650	9	50	MTX	0.005	0.0001	0.0001
<i>p</i> ABA-caproic hydroxamic acid (5)	650	9	50							
MTX	0.005	0.0001	0.0001							

**Fig. (2).** Molecular docking of folate-*p*ABA-caproic hydroxamic acid (4) into the active-site pocket of human recombinant HDAC8 (left) and methotrexate-caproic hydroxamic acid (2) into *Lactobacillus casei* DHFR (right).

case of DHFR. Therefore, the same procedure was used for the docking of the synthesized ligands inside the active site of the two enzymes.

In order to gain insight into the binding mode of the most potent inhibitor in HDAC8 active site, a docking approach was employed using as a model the catalytic core of human HDAC8 (Fig. 2. left). This inhibitor (4) is able to accommodate its long aliphatic chain into the enzyme's pocket and make several contacts with the tube-link hydrophobic portion of the pocket establishing good interactions. The terminal hydroxamic acid group reaches the polar bottom of the pocket where it coordinates the zinc ion in a bidentate fashion while interacting simultaneously with His142 and His143, residues likely to be involved the catalytic process [25, 26]. In the ligand chain connecting the linker and the cap group, the amide function establishes a strong hydrogen bond with Asp101 (1.99 Å). The aromatic cap group of this ligand consists of a phenyl-amino group that interacts with the Tyr100 residue by a hydrogen bond (2.04 Å). An additional significant hydrogen bond is formed between the

pteridine amine group and Asp101 (2.07 Å). Due to the conformational arrangement in this inhibitor, it interacts in a suitable manner with the hydrophobic residues of the outside surface of the protein. The presence of this  $\pi$ - $\pi$  interaction between a phenyl moiety of the inhibitor and the Tyr100 residue, contributes to increase the favorable interactions with the enzyme's surface. The additional hydrogen bond contributes to the enhanced binding of the pteridine ring, which otherwise is retained by non-hydrophobic interactions with residues on the outer surface of the enzyme.

The same approach was used to assess the binding mode of the most potent derivative (2) into DHFR active site (Fig. 2. right). For this docking calculation, a model of the catalytic core of *L. casei* DHFR was used. Inhibitors of DHFR usually include a 2,4-diamino substitution in the pteridine ring which binds to DHFR active site establishing important hydrogen bonds with the Asp26 (1.88 Å), Ala97 (2.40 Å) and Leu4 (1.55 Å) amino acid residues. Some significant interactions can also be observed between the pteridine ring of the MTX derivative and the hydrophobic portion of the

enzyme active site. Furthermore, the presence of  $\pi$ - $\pi$  interaction between this planar moiety and Phe30 should give an important contribution to the good inhibition values found for this derivative. Additional hydrogen bond interactions can be found between the carboxylic oxygen atoms present in the flexible moiety of this inhibitor and the amino acid residues Arg57 and His28. In conclusion, all these favorable interactions between the inhibitor and the amino acid residues contribute to enclose it successfully into the active site and, consequently, obtain satisfactory inhibition values.

## CONCLUSIONS

A set of novel hybrid compounds, namely hydroxamate derivatives of methotrexate (MTX) and folic acid, have been developed and evaluated for their ability to inhibit HDAC8 and DHFR, two enzymes with important roles in tumor cells. The anti-proliferative activity of the compounds in two cancer cell lines (lung carcinoma and human prostate adenocarcinoma) was further evaluated.

The folate and MTX derivatives showed a reasonably good ability to inhibit both HDAC and DHFR. With regard to HDAC inhibition, folate-*p*ABA-caproic hydroxamic acid (**4**) was the most active; despite its large size, it can form strong interactions with the enzyme catalytic site. This inhibition is quite independent of the pteridine-ring 4-substituent (amino for MTX; hydroxyl for folic acid). Concerning the DHFR inhibition and the antiproliferative effects on lung carcinoma cells, the MTX derivative **2** was the most active compound, as expected. Thus, it can be hypothesized that if some of the derivatizations made on folic acid (e.g. compound **3** and **4**) were extended to MTX, it would result on MTX derivatives with high inhibitory activity against both DHFR and HDAC8. The fact that the studied derivatives retain the capability to inhibit two independent targets provides directions for design strategies of novel hybrid compounds with improved dual activity against HDACs and DHFR and for improved treatment of cancer including metastasizing tumors.

## EXPERIMENTAL

### Chemicals and Equipment

All the commercially available reagents were of the highest purity and were used without further purifications. Folic acid, methotrexate, *O*-benzotriazol-1-yl-*N,N,N',N'*-tetramethyluronium-tetrafluoroborate (TBTU), *N*-methylmorpholine (redistilled),  $\text{NH}_2\text{OH}$ , di-*tert*-butyl dicarbonate were purchased from *Sigma-Aldrich* and 6-amino-caproic acid, 4-amino-benzoic acid from *Acros Organics*. The solvents were purchased from *Acros Organics* or *Merck* and, whenever necessary, they were purified and dried according to standard methods [27]. All moisture-sensitive reactions were performed under nitrogen atmosphere. The chemical reactions were followed by TLC using silica gel plates (G-60 F<sub>254</sub>, Merck). A Bio-Rad Merlin, FTS 3000 MX spectrometer was used to record solid state IR spectra (KBr pellets). <sup>1</sup>H and <sup>13</sup>C NMR spectra were recorded on a Varian Unity 300 FT NMR spectrometer at 25 °C. If necessary, assignment of the signals of the <sup>13</sup>C NMR signals were confirmed by DEPT. Chemical shifts are reported in ppm ( $\delta$ )

from sodium 3-(trimethylsilyl)-[2,2,3,3-<sup>2</sup>H<sub>4</sub>]-propionate as internal reference in D<sub>2</sub>O solutions. The following abbreviations are used: d = doublet; s = singlet; t = triplet; m = multiplet; br = broad. Mass spectra (FAB) were performed on a VG TRIO-2000 GCMS instrument. High Resolution Mass Spectrometry (HRMS (ESI)) measurements were performed on an APEX III FT-ICR MS (Bruker Daltonics, Billerica, MA), equipped with a 7T actively shielded magnet. Ions were generated using an Apollo API electrospray ionization (ESI) source. Ionization was achieved by an electrospray ionization source (Bruker Daltonics, Billerica, MA), with a voltage of between 1800 and 2200 V (to optimize ionization efficiency) applied to the needle, and a counter voltage of 450 V applied to the capillary. Samples were prepared by adding a spray solution of 70:29.5:0.5 (v/v/v) CH<sub>3</sub>OH/water/formic acid to a solution of the sample at a v/v ratio of 1 to 5% to give the best signal-to-noise ratio. Data acquisition and data processing were performed using the XMASS software, version 6.1.2 (Bruker Daltonics). Elemental analyses were performed on a Fisons EA 1108 CHN/O instrument.

### Synthesis

(*S*)-6-(4-(4-(((2-Amino-4-hydroxypteridin-6-yl)methyl)amino)benzamido)-4-carboxybutanamido)hexanoic acid (Folate-caproic acid, **6**).

A first solution mixture was prepared by adding *N*-methylmorpholine (0.048 mL, 0.44 mmol) to a solution of folic acid (0.100 g, 0.22 mmol) in dry DMF (10 mL) under nitrogen and this solution was cooled in an ice bath at 0 °C followed by the addition of TBTU (0.071 g, 0.22 mmol). This solution was slowly added to a water-ice cooled solution of 6-amino caproic acid (0.036 g, 0.22 mmol) in dry DMF (10 mL) and the reaction mixture was stirred for 2 h at 0 °C and then it was left to heat up to RT and left stirring for 12 h. DMF was evaporated under high vacuum. Recrystallization of the solid residue from a mixture of dry dichloromethane/ethanol provided the pure product as yellow crystals (67%); <sup>1</sup>H NMR (D<sub>2</sub>O, pD = ca. 9)  $\delta$ : 8.59 (1H, s, CH=N), 6.80 (2H, d, CH=C-NH), 7.65 d (2H, d, CH=C-C=O), 4.57 (2H, s, CH<sub>2</sub>-NH), 4.34 (1H, s, CH-COOH), 2.91 (2H, t, NH-CH<sub>2</sub>-CH<sub>2</sub>-CH<sub>2</sub>-CH<sub>2</sub>-CH<sub>2</sub>), 2.31 (2H, t, CH<sub>2</sub>-C=O), 2.14 (2H, t, NH-CH<sub>2</sub>-CH<sub>2</sub>-CH<sub>2</sub>-CH<sub>2</sub>-CH<sub>2</sub>), 2.04 (2H, d, CH<sub>2</sub>-CH), 1.45 (4H, m, NH-CH<sub>2</sub>-CH<sub>2</sub>-CH<sub>2</sub>-CH<sub>2</sub>-CH<sub>2</sub>-NH-CH<sub>2</sub>-CH<sub>2</sub>-CH<sub>2</sub>-CH<sub>2</sub>-CH<sub>2</sub>-CH<sub>2</sub>), 1.18 (2H, q, NH-CH<sub>2</sub>-CH<sub>2</sub>-CH<sub>2</sub>-CH<sub>2</sub>-CH<sub>2</sub>-CH<sub>2</sub>); IR: 1541 cm<sup>-1</sup> ( $\nu_{\text{NH}(\text{CONH})}$ , new amide bond); MS (FAB) m/z: 555 (50%) (M+1).

(*S*)-2-(4-(((2-Amino-4-hydroxypteridin-6-yl)methyl)amino)benzamido)-5-((6-(hydroxyamino)-6-oxohexyl)amino)-5-oxopentanoic acid (Folate-caproic hydroxamic acid, **1**).

A cooled solution mixture containing the activated folate-caproic acid was slowly added to a water-ice cooled solution of the free hydroxylamine prepared under nitrogen, by adding potassium hydroxide as pellets (0.05 g, 0.85 mmol) to a solution of hydroxylamine hydrochloride (0.06 g, 0.85 mmol) in dry DMF (10 mL), containing activated molecular sieves (0.4 nm, Riedel-de Haën), in an ice bath at 0 °C. The mixture was stirred for 30 min and the inorganic solids were filtered out from the solution. The first solution was added slowly to the second one and the mixture was left stirring for

5 h at 0 °C and the solution was kept at this temperature for 12 h. After evaporation of the solvent (DMF) under high vacuum, the solid residue was taken into CH<sub>2</sub>Cl<sub>2</sub> and by the addition of dry ethanol solids were precipitated, filtered and washed with ethanol and diethyl ether in the end. Recrystallization of these solid from DMF provided yellow crystals as pure product (83%); m.p. 250-260 °C (decomposition). <sup>1</sup>H NMR (D<sub>2</sub>O, pD ca. 9) δ: 8.62 (1H, s, CH=N), 7.68 d (2H, d, CH=C=O), 6.86 (2H, d, CH=C-NH), 4.62 (2H, s, CH<sub>2</sub>-NH), 4.33 (1H, s, CH-COOH), 2.97 (2H, t, NH-CH<sub>2</sub>-CH<sub>2</sub>-CH<sub>2</sub>-CH<sub>2</sub>-CH<sub>2</sub>), 2.33 (2H, t, CH<sub>2</sub>-C=O), 2.15 (2H, t, NH-CH<sub>2</sub>-CH<sub>2</sub>-CH<sub>2</sub>-CH<sub>2</sub>-CH<sub>2</sub>), 2.06 (2H, d, CH<sub>2</sub>-CH), 1.54 (4H, m, NH-CH<sub>2</sub>-CH<sub>2</sub>-CH<sub>2</sub>-CH<sub>2</sub>-CH<sub>2</sub>, NH-CH<sub>2</sub>-CH<sub>2</sub>-CH<sub>2</sub>-CH<sub>2</sub>-CH<sub>2</sub>), 1.29 (2H, q, NH-CH<sub>2</sub>-CH<sub>2</sub>-CH<sub>2</sub>-CH<sub>2</sub>-CH<sub>2</sub>); <sup>13</sup>C NMR (DEPT) (D<sub>2</sub>O, pD = ca. 9) δ: 150 (CH=N), 132 (CH=C=O), 115 (CH=C-NH), 57.5 (CH-COOH), 48.2 (CH<sub>2</sub>-NH), 41.8 (NH-CH<sub>2</sub>-CH<sub>2</sub>-CH<sub>2</sub>-CH<sub>2</sub>-CH<sub>2</sub>), 39.9 (NH-CH<sub>2</sub>-CH<sub>2</sub>-CH<sub>2</sub>-CH<sub>2</sub>-CH<sub>2</sub>), 35.0 (CH<sub>2</sub>-C=O), 30.3 (CH<sub>2</sub>-CH), 28.4 (NH-CH<sub>2</sub>-CH<sub>2</sub>-CH<sub>2</sub>-CH<sub>2</sub>-CH<sub>2</sub>), 27.9 (NH-CH<sub>2</sub>-CH<sub>2</sub>-CH<sub>2</sub>-CH<sub>2</sub>-CH<sub>2</sub>), 27.3 (NH-CH<sub>2</sub>-CH<sub>2</sub>-CH<sub>2</sub>-CH<sub>2</sub>-CH<sub>2</sub>); IR: 1614 cm<sup>-1</sup> (ν<sub>C=O</sub>, new amide bond) 1547 cm<sup>-1</sup>, 1521 cm<sup>-1</sup> (ν<sub>NH(CONH)</sub>, new amide bond). Anal. found: C, 52.92; H, 5.63; N, 22.20%; calculated for C<sub>25</sub>H<sub>31</sub>N<sub>9</sub>O<sub>7</sub>: C, 52.72; H, 5.49; N, 22.13%.

(S)-6-(4-Carboxy-4-(((2,4-diaminopteridin-6-yl)methyl)(methyl)amino)benzamido)butanamido) hexanoic acid (Methotrexate-caproic acid, 7).

From MTX and 6-amino-caproic acid, as in the case of folate-caproic acid. Yellow crystals (24%); <sup>1</sup>H NMR (D<sub>2</sub>O, pD = ca. 9) δ: 8.55 (1H, s, CH=N), 7.65 d (2H, d, CH=C=O), 6.84 (2H, d, CH=C-NH), 4.80 (2H, s, CH<sub>2</sub>-NCH<sub>3</sub>), 4.37 (1H, s, CH-COOH), 3.16 (3H, s, CH<sub>3</sub>), 2.84 (2H, t, NH-CH<sub>2</sub>-CH<sub>2</sub>-CH<sub>2</sub>-CH<sub>2</sub>-CH<sub>2</sub>), 2.30 (2H, t, CH<sub>2</sub>-C=O), 2.10 (2H, t, NH-CH<sub>2</sub>-CH<sub>2</sub>-CH<sub>2</sub>-CH<sub>2</sub>-CH<sub>2</sub>), 1.98 (2H, d, CH<sub>2</sub>-CH), 1.49 (4H, m, NH-CH<sub>2</sub>-CH<sub>2</sub>-CH<sub>2</sub>-CH<sub>2</sub>-CH<sub>2</sub>, NH-CH<sub>2</sub>-CH<sub>2</sub>-CH<sub>2</sub>-CH<sub>2</sub>-CH<sub>2</sub>), 1.17 (2H, q, NH-CH<sub>2</sub>-CH<sub>2</sub>-CH<sub>2</sub>-CH<sub>2</sub>-CH<sub>2</sub>); <sup>13</sup>C NMR (DEPT) (DMSO-d<sub>6</sub>) δ: 147 (CH=N), 129 (CH=C=O), 111 (CH=C-NH), 54.6 (CH-COOH), 52.8 (CH<sub>2</sub>-NCH<sub>3</sub>), 32.1 (CH<sub>2</sub>-C=O), 28.9 (NH-CH<sub>2</sub>-CH<sub>2</sub>-CH<sub>2</sub>-CH<sub>2</sub>-CH<sub>2</sub>), 27.2 (CH<sub>2</sub>-CH), 26.0 (NH-CH<sub>2</sub>-CH<sub>2</sub>-CH<sub>2</sub>-CH<sub>2</sub>-CH<sub>2</sub>), 24.3 (NH-CH<sub>2</sub>-CH<sub>2</sub>-CH<sub>2</sub>-CH<sub>2</sub>-CH<sub>2</sub>), covered by the solvent peak (CH<sub>3</sub>, NH-CH<sub>2</sub>-CH<sub>2</sub>-CH<sub>2</sub>-CH<sub>2</sub>-CH<sub>2</sub>, NH-CH<sub>2</sub>-CH<sub>2</sub>-CH<sub>2</sub>-CH<sub>2</sub>-CH<sub>2</sub>); IR: 1646 cm<sup>-1</sup> (ν<sub>C=O</sub>, new amide bond); MS (FAB) m/z: 568 (100%) (M+1).

(S)-2-(4-(((2,4-Diaminopteridin-6-yl)methyl)(methyl)amino)benzamido)-5-((6-(hydroxyamino)-6-oxohexyl)amino)-5-oxopentanoic acid (Methotrexate-caproic hydroxamic acid, 2).

From methotrexate-caproic acid, as in the case of methotrexate-caproic hydroxamic acid. Yellow crystals (36%); m.p. 153-155 °C. <sup>1</sup>H NMR (D<sub>2</sub>O, pD ca. 9) δ: 8.59 (1H, s, CH=N), 7.68 d (2H, d, CH=C=O), 6.88 (2H, d, CH=C-NH), 4.55 (2H, s, CH<sub>2</sub>-NCH<sub>3</sub>), 4.40 (1H, s, CH-COOH), 3.18 (3H, s, CH<sub>3</sub>), 2.85 (2H, t, NH-CH<sub>2</sub>-CH<sub>2</sub>-CH<sub>2</sub>-CH<sub>2</sub>-CH<sub>2</sub>), 2.32 (2H, t, CH<sub>2</sub>-C=O), 2.11 (2H, t, NH-CH<sub>2</sub>-CH<sub>2</sub>-CH<sub>2</sub>-CH<sub>2</sub>-CH<sub>2</sub>), 1.99 (2H, d, CH<sub>2</sub>-CH), 1.49 (4H, m, NH-CH<sub>2</sub>-CH<sub>2</sub>-CH<sub>2</sub>-CH<sub>2</sub>-CH<sub>2</sub>, NH-CH<sub>2</sub>-CH<sub>2</sub>-CH<sub>2</sub>-CH<sub>2</sub>-CH<sub>2</sub>), 1.18 (2H, q, NH-CH<sub>2</sub>-CH<sub>2</sub>-CH<sub>2</sub>-CH<sub>2</sub>-CH<sub>2</sub>); <sup>13</sup>C NMR (DEPT) (D<sub>2</sub>O, pD = ca. 10) δ: 151 (CH=N), 131 (CH=C=O), 114 (CH=C-NH), 57.4 (CH<sub>2</sub>-NCH<sub>3</sub>), 55.0 (CH-

COOH), 41.7 (NH-CH<sub>2</sub>-CH<sub>2</sub>-CH<sub>2</sub>-CH<sub>2</sub>-CH<sub>2</sub>), 39.9 (CH<sub>3</sub>), 35.2 (NH-CH<sub>2</sub>-CH<sub>2</sub>-CH<sub>2</sub>-CH<sub>2</sub>-CH<sub>2</sub>), 33.2 (CH<sub>2</sub>-C=O), 30.2 (NH-CH<sub>2</sub>-CH<sub>2</sub>-CH<sub>2</sub>-CH<sub>2</sub>-CH<sub>2</sub>), 28.5 (NH-CH<sub>2</sub>-CH<sub>2</sub>-CH<sub>2</sub>-CH<sub>2</sub>-CH<sub>2</sub>), 27.9 (NH-CH<sub>2</sub>-CH<sub>2</sub>-CH<sub>2</sub>-CH<sub>2</sub>-CH<sub>2</sub>), 27.4 (CH<sub>2</sub>-CH); IR: 1644 cm<sup>-1</sup> (ν<sub>C=O</sub>, new amide bond). Anal. found: C, 53.49; H, 5.92; N, 24.23%; calculated for C<sub>26</sub>H<sub>34</sub>N<sub>10</sub>O<sub>6</sub>: C, 53.60; H, 6.03; N, 24.04%.

(S)-4-(4-(4-(((2-Amino-4-hydroxypteridin-6-yl)methyl)amino)benzamido)-4-carboxybutanamido) benzoic acid (Folate-pABA, 8).

From folic acid and pABA, as in the case of folate-caproic acid. Yellow crystals (62%); <sup>1</sup>H NMR (D<sub>2</sub>O, pD ca. 9) δ: 8.51 (1H, s, CH=N), 7.65 d (2H, d, CH=C=O), 7.44 (2H, d, NH-C=CH(pABA)), 7.25 (2H, d, CH=C-CO(pABA)), 6.63 (2H, d, CH=C-NH), 4.49 (2H, s, CH<sub>2</sub>-NH), 4.42 (1H, s, CH-COOH), 2.36 (2H, t, CH<sub>2</sub>-C=O), 2.31 (2H, d, CH<sub>2</sub>-CH); <sup>13</sup>C NMR (DEPT) (D<sub>2</sub>O, pD = ca. 9) δ: 150 (CH=N), 132 (CH=C-CO(pABA)), 131 (CH=C=O), 124 (NH-C=CH(pABA)), 115 (CH=C-NH), 57.7 (CH-COOH), 48.4 (CH<sub>2</sub>-NH), 36.2 (CH<sub>2</sub>-C=O), 30.2 (CH<sub>2</sub>-CH); IR: 1654 cm<sup>-1</sup> (ν<sub>C=O</sub>, new amide bond), 1540 cm<sup>-1</sup>, 1510 cm<sup>-1</sup> (ν<sub>NH(CONH)</sub>, new amide bond); MS (FAB) m/z: 561 (85%) (M+1).

(S)-2-(4-(((2-Amino-4-hydroxypteridin-6-yl)methyl)amino)benzamido)-5-((4-(hydroxycarbamoyl)phenyl)amino)-5-oxopentanoic acid (Folate-pABA hydroxamic acid, 3).

From folate-pABA, as in the case of folate-caproic hydroxamic acid. Yellow crystals (92%); m.p. 210-220 °C (decomposition). <sup>1</sup>H NMR (D<sub>2</sub>O, pD = ca. 9) δ: 8.53 (1H, s, CH=N), 7.64 d (2H, d, CH=C=O), 7.49 (2H, d, NH-C=CH(pABA)), 7.30 (2H, d, CH=C-CO(pABA)), 6.68 (2H, d, CH=C-NH), 4.52 (2H, s, CH<sub>2</sub>-NH), 4.46 (1H, s, CH-COOH), 2.17 (2H, t, CH<sub>2</sub>-C=O), 2.11 (2H, d, CH<sub>2</sub>-CH); <sup>13</sup>C NMR (DEPT) (D<sub>2</sub>O, pD = ca. 9) δ: 150 (CH=N), 132 (CH=C-CO(pABA)), 131 (CH=C=O), 123 (NH-C=CH(pABA)), 115 (CH=C-NH), 57.9 (CH-COOH), 48.4 (CH<sub>2</sub>-NH), 33.9 (CH<sub>2</sub>-C=O), 30.1 (CH<sub>2</sub>-CH); IR: 1658 cm<sup>-1</sup> (ν<sub>C=O</sub>, new amide bond), 1539 cm<sup>-1</sup>, 1514 cm<sup>-1</sup> (ν<sub>NH(CONH)</sub>, new amide bond). Anal. found: C, 53.41; H, 4.59; N, 21.76%; calculated for C<sub>26</sub>H<sub>25</sub>N<sub>9</sub>O<sub>7</sub>: C, 53.26; H, 4.38; N, 21.90%.

(S)-6-(4-(4-(4-(((2-Amino-4-hydroxypteridin-6-yl)methyl)amino)benzamido)-4-carboxybutanamido) benzamido)hexanoic acid (Folate-pABA-caproic acid, 9).

From folate-pABA and 6-amino-caproic acid, as in the case of folate-caproic acid. Yellow crystals (66%); <sup>1</sup>H NMR (D<sub>2</sub>O, pD = ca. 9) δ: 8.56 (1H, s, CH=N), 7.84 (2H, d, CH=C-CO(pABA)), 7.67 (2H, d, NH-C=CH(pABA)), 7.51 d (2H, d, CH=C=O), 6.78 (2H, d, CH=C-NH), 4.58 (2H, s, CH<sub>2</sub>-NH), 4.38 (1H, s, CH-COOH), 3.00 (2H, t, NH-CH<sub>2</sub>-CH<sub>2</sub>-CH<sub>2</sub>-CH<sub>2</sub>-CH<sub>2</sub>), 2.40 (2H, t, CH<sub>2</sub>-C=O), 2.12 (4H, m, CH<sub>2</sub>-CH, NH-CH<sub>2</sub>-CH<sub>2</sub>-CH<sub>2</sub>-CH<sub>2</sub>-CH<sub>2</sub>), 1.48 (6H, br, NH-CH<sub>2</sub>-CH<sub>2</sub>-CH<sub>2</sub>-CH<sub>2</sub>-CH<sub>2</sub>, NH-CH<sub>2</sub>-CH<sub>2</sub>-CH<sub>2</sub>-CH<sub>2</sub>-CH<sub>2</sub>); <sup>13</sup>C NMR (DEPT) (D<sub>2</sub>O, pD = ca. 9) δ: 150 (CH=N), 132 (CH=C-CO(pABA)), 131 (CH=C=O), 123 (NH-C=CH(pABA)), 114 (CH=C-NH), 57.8 (CH-COOH), 48.2 (CH<sub>2</sub>-NH), 39.9 (NH-CH<sub>2</sub>-CH<sub>2</sub>-CH<sub>2</sub>-CH<sub>2</sub>-CH<sub>2</sub>), 36.3 (CH<sub>2</sub>-C=O), 30.2 (CH<sub>2</sub>-CH), 41.8 (NH-CH<sub>2</sub>-CH<sub>2</sub>-CH<sub>2</sub>-CH<sub>2</sub>-CH<sub>2</sub>), 29.3 (NH-CH<sub>2</sub>-CH<sub>2</sub>-

CH<sub>2</sub>-CH<sub>2</sub>-CH<sub>2</sub>), 28.4 (NH-CH<sub>2</sub>-CH<sub>2</sub>-CH<sub>2</sub>-CH<sub>2</sub>-CH<sub>2</sub>), 28.1 (NH-CH<sub>2</sub>-CH<sub>2</sub>-CH<sub>2</sub>-CH<sub>2</sub>-CH<sub>2</sub>); IR: 1641 cm<sup>-1</sup> (ν<sub>C=O</sub>, new amide bond), 1538 cm<sup>-1</sup>, 1513 cm<sup>-1</sup> (ν<sub>NH(CONH)</sub>, new amide bond); MS (FAB) m/z: 674 (20%) (M+1).

*(S)*-2-(4-(((2-Amino-4-hydroxypteridin-6-yl)methyl)amino)benzamido)-5-((4-((6-(hydroxyamino)-6-oxohexyl)carbamoyl)phenyl)amino)-5-oxopentanoic acid (*Folate-pABA-caproic hydroxamic acid, 4*).

From folate-*pABA*-caproic acid, as in the case of folate-caproic hydroxamic acid. Yellow crystals (65%); m.p. 260-270 °C (decomposition). <sup>1</sup>H NMR (D<sub>2</sub>O, pD = ca. 9) δ: 8.57 (1H, s, CH=N), 7.66 (2H, d, NH-C=CH(*pABA*)), 7.52 d (2H, d, CH=C-C=O), 7.26 (2H, d, CH=C-CO(*pABA*)), 6.80 (2H, d, CH=C-NH), 4.58 (2H, s, CH<sub>2</sub>-NH), 4.40 (1H, s, CH-COOH), 3.00 (2H, t, NH-CH<sub>2</sub>-CH<sub>2</sub>-CH<sub>2</sub>-CH<sub>2</sub>-CH<sub>2</sub>), 2.45 (2H, t, CH<sub>2</sub>-C=O), 2.11 (4H, m, CH<sub>2</sub>-CH, NH-CH<sub>2</sub>-CH<sub>2</sub>-CH<sub>2</sub>-CH<sub>2</sub>-CH<sub>2</sub>), 1.35 (6H, br, NH-CH<sub>2</sub>-CH<sub>2</sub>-CH<sub>2</sub>-CH<sub>2</sub>-CH<sub>2</sub>, NH-CH<sub>2</sub>-CH<sub>2</sub>-CH<sub>2</sub>-CH<sub>2</sub>-CH<sub>2</sub>, NH-CH<sub>2</sub>-CH<sub>2</sub>-CH<sub>2</sub>-CH<sub>2</sub>-CH<sub>2</sub>); <sup>13</sup>C NMR (DEPT) (D<sub>2</sub>O, pD ca. 9) δ: 150 (CH=N), 132 (CH=C-CO(*pABA*)), 131 (CH=C-C=O), 124 (NH-C=CH(*pABA*)), 115 (CH=C-NH), 57.3 (CH-COOH), 48.2 (CH<sub>2</sub>-NH), 41.8 (NH-CH<sub>2</sub>-CH<sub>2</sub>-CH<sub>2</sub>-CH<sub>2</sub>-CH<sub>2</sub>), 39.9 (NH-CH<sub>2</sub>-CH<sub>2</sub>-CH<sub>2</sub>-CH<sub>2</sub>-CH<sub>2</sub>), 35.0 (CH<sub>2</sub>-C=O), 30.6 (CH<sub>2</sub>-CH), 28.5 (NH-CH<sub>2</sub>-CH<sub>2</sub>-CH<sub>2</sub>-CH<sub>2</sub>-CH<sub>2</sub>), 27.9 (NH-CH<sub>2</sub>-CH<sub>2</sub>-CH<sub>2</sub>-CH<sub>2</sub>-CH<sub>2</sub>), 27.5 (NH-CH<sub>2</sub>-CH<sub>2</sub>-CH<sub>2</sub>-CH<sub>2</sub>-CH<sub>2</sub>); IR: 1640 cm<sup>-1</sup> (ν<sub>C=O</sub>, new amide bond), 1536 cm<sup>-1</sup>, 1511 cm<sup>-1</sup> (ν<sub>NH(CONH)</sub>, new amide bond). Anal. found: C, 55.63; H, 5.3; N, 20.56%; calculated for C<sub>32</sub>H<sub>36</sub>N<sub>10</sub>O<sub>8</sub>: C, 55.81; H, 5.27; N, 20.34%.

*4-((Tert-butoxycarbonyl)amino)benzoic acid (Boc-pABA, 10)*.

A solution mixture of *pABA* (1.03 g, 7.5 mmol) in water (8 mL) and 1,4-dioxane (8 mL) was cooled in an ice bath at 0 °C followed by the parallel addition of Na<sub>2</sub>CO<sub>3</sub> (1.53 g, 15 mmol) in water (10 mL) and di-*tert*-butyl-dicarbonate (Boc<sub>2</sub>O) (1.80 g, 8.25 mmol) in 1,4-dioxane (10 mL). The reaction mixture was stirred for 4 h at 0 °C and then it was left to heat up to RT overnight. The pH of the solution was decreased to pH = 2 with 2 M HCl and a white solid was precipitated as the product, which was filtered off and washed with large amount of HCl solution to get the pure product as white crystals (95%); m.p. 205-206 °C. <sup>1</sup>H NMR (acetone-*d*<sub>6</sub>) δ: 7.85 (2H, d, CH=C-CO), 7.39 (2H, d, NH-C=CH), 1.51 (9H, s, C(CH<sub>3</sub>)<sub>3</sub>); IR: 3390, 3423, 3484, 3566 cm<sup>-1</sup> (ν<sub>NH</sub>).

*6-(4-((Tert-butoxycarbonyl)amino)benzamido)hexanoic acid (Boc-pABA-caproic acid, 11)*.

From Boc-*pABA* and 6-amino-caproic acid, as in the case of folate-caproic acid, but after the evaporation of the solvent DMF the solid residue was taken into a mixture of H<sub>2</sub>O and CH<sub>2</sub>Cl<sub>2</sub> at neutral pH and the insoluble solid was identified as the product. Recrystallization from methanol provided the pure product as white crystals (78%); m.p. 143 °C. <sup>1</sup>H NMR (MeOD) δ: 7.61 (2H, d, CH=C-CO), 7.35 (2H, d, NH-C=CH), 3.30 (2H, t, NH-CH<sub>2</sub>-CH<sub>2</sub>-CH<sub>2</sub>-CH<sub>2</sub>-CH<sub>2</sub>), 2.14 (2H, t, NH-CH<sub>2</sub>-CH<sub>2</sub>-CH<sub>2</sub>-CH<sub>2</sub>-CH<sub>2</sub>), 1.54 (4H, m, NH-CH<sub>2</sub>-CH<sub>2</sub>-CH<sub>2</sub>-CH<sub>2</sub>-CH<sub>2</sub>, NH-CH<sub>2</sub>-CH<sub>2</sub>-CH<sub>2</sub>-CH<sub>2</sub>-CH<sub>2</sub>), 1.44 (9H, s, C(CH<sub>3</sub>)<sub>3</sub>), 1.32 (2H, q, NH-CH<sub>2</sub>-CH<sub>2</sub>-CH<sub>2</sub>-CH<sub>2</sub>-CH<sub>2</sub>).

*Tert-butyl (4-((6-(hydroxyamino)-6-oxohexyl)carbamoyl)phenyl)carbamate (Boc-pABA-caproic hydroxamic acid, 12)*.

From Boc-*pABA*-caproic acid, as in the case of folate-caproic hydroxamic acid, but after the evaporation of the solvent DMF the solid residue was taken into H<sub>2</sub>O and the insoluble solid was identified as the product. Recrystallization from CH<sub>3</sub>CN provided the pure product as white crystals (88%); m.p. 133 °C. <sup>1</sup>H NMR (MeOD) δ: 7.67 (2H, d, CH=C-CO), 7.38 (2H, d, NH-C=CH), 3.33 (2H, t, NH-CH<sub>2</sub>-CH<sub>2</sub>-CH<sub>2</sub>-CH<sub>2</sub>-CH<sub>2</sub>), 2.04 (2H, t, NH-CH<sub>2</sub>-CH<sub>2</sub>-CH<sub>2</sub>-CH<sub>2</sub>-CH<sub>2</sub>), 1.58 (4H, m, NH-CH<sub>2</sub>-CH<sub>2</sub>-CH<sub>2</sub>-CH<sub>2</sub>-CH<sub>2</sub>, NH-CH<sub>2</sub>-CH<sub>2</sub>-CH<sub>2</sub>-CH<sub>2</sub>-CH<sub>2</sub>), 1.47 (9H, s, C(CH<sub>3</sub>)<sub>3</sub>), 1.32 (2H, q, NH-CH<sub>2</sub>-CH<sub>2</sub>-CH<sub>2</sub>-CH<sub>2</sub>-CH<sub>2</sub>). MS (FAB) m/z: 689 (M+1).

*4-Amino-N-(6-(hydroxyamino)-6-oxohexyl)benzamide (pABA-caproic hydroxamic acid, 5)*.

Boc-*pABA*-caproic hydroxamic acid (3.01 g, 4.50 mmoles) was dissolved in a mixture of 20 % of trifluoroacetic acid (TFA) in CH<sub>2</sub>Cl<sub>2</sub> (40 mL) and was left stirring for 4 h. Then the solvents were evaporated and recrystallization from methanol provided the pure product as white crystals (22%); m.p. 43 °C. <sup>1</sup>H NMR (D<sub>2</sub>O) δ: 7.58 (2H, d, CH=C-CO), 6.83 (2H, d, NH-C=CH), 3.33 (2H, t, NH-CH<sub>2</sub>-CH<sub>2</sub>-CH<sub>2</sub>-CH<sub>2</sub>-CH<sub>2</sub>), 2.05 (2H, t, NH-CH<sub>2</sub>-CH<sub>2</sub>-CH<sub>2</sub>-CH<sub>2</sub>-CH<sub>2</sub>), 1.59 (4H, m, NH-CH<sub>2</sub>-CH<sub>2</sub>-CH<sub>2</sub>-CH<sub>2</sub>-CH<sub>2</sub>, NH-CH<sub>2</sub>-CH<sub>2</sub>-CH<sub>2</sub>-CH<sub>2</sub>-CH<sub>2</sub>), 1.35 (2H, q, NH-CH<sub>2</sub>-CH<sub>2</sub>-CH<sub>2</sub>-CH<sub>2</sub>-CH<sub>2</sub>); <sup>13</sup>C NMR (DEPT) (D<sub>2</sub>O) δ: 131 (CH=C-CO), 126 (NH<sub>2</sub>-C=CH), 42.3 (NH-CH<sub>2</sub>-CH<sub>2</sub>-CH<sub>2</sub>-CH<sub>2</sub>-CH<sub>2</sub>), 34.0 (NH-CH<sub>2</sub>-CH<sub>2</sub>-CH<sub>2</sub>-CH<sub>2</sub>-CH<sub>2</sub>), 30.5 (NH-CH<sub>2</sub>-CH<sub>2</sub>-CH<sub>2</sub>-CH<sub>2</sub>-CH<sub>2</sub>), 27.9 (NH-CH<sub>2</sub>-CH<sub>2</sub>-CH<sub>2</sub>-CH<sub>2</sub>-CH<sub>2</sub>), 27.6 (NH-CH<sub>2</sub>-CH<sub>2</sub>-CH<sub>2</sub>-CH<sub>2</sub>-CH<sub>2</sub>); IR: 1626 cm<sup>-1</sup> (ν<sub>C=O</sub>); MS (FAB) m/z: 266 (M+1). Anal. found: C, 58.92; H, 7.19; N, 15.97%; calculated for C<sub>13</sub>H<sub>19</sub>N<sub>3</sub>O<sub>3</sub>: C, 58.85; H, 7.22; N, 16.13%.

## HDAC Inhibition Assays

The bioassay for HDAC8 activity was performed using an HDAC fluorescence activity assay/drug discovery kit (CycLex<sup>®</sup> HDAC8 Deacetylase Fluorometric Assay Kit) according to the manufacturer's recommendation. The assay measures the activity of HDAC8 towards a fluoro-substrate containing acetylated lysine side chains. The buffer for substrate, enzymes and inhibitors was 20 mM Tris-HCl, pH 8.0, 125 mM NaCl, 1% glycerol. Human recombinant HDAC8 (10 μL) enzyme was incubated in buffer for 10 min at 25 °C in the presence of fluoro-substrate (20 μM), lysyl endopeptidase (0.25 mAU/mL) and different inhibitor concentrations (from 0.1 to 200 μM) in DMSO (5 μL), in a total volume of 50 μL in 96 well flat-bottomed plates. After incubation, the reactions gave a stable fluorescence signal for up to 60 min. The fluorescence of each reaction was measured on a fluorometric reader (Molecular Device SpectraMax Gemini XS plate reader) at 37 °C with excitation at 340 nm and emission at 440 nm. The percent inhibition was calculated from the fluorescence reading of the inhibited reaction relative to the control reaction with buffer (5 μL) in place of inhibitor. As reference, control Trichostatin A was used (5 μL, 20 μM) to have a 100% inhibition. All of the assays were performed in duplicate, and all of the values were used for calculation of IC<sub>50</sub>. The HDAC8 inhibition activity was expressed in relative fluorescent units. Percent of inhibition

was calculated from control reactions without the inhibitor.  $IC_{50}$  was determined using the formula:  $v_i/v_0 = 1/(1 + [I]/IC_{50})$ , where  $v_i$  is the initial velocity of substrate cleavage in the presence of the inhibitor at concentration  $[I]$  and  $v_0$  is the initial velocity in the absence of the inhibitor. Results were analyzed using SoftMax Pro software and GraFit software [28,29].

The assay for HDAC activity in crude nuclear extract from HeLa was performed using an HDAC fluorescence activity assay/drug discovery kit (CycLex<sup>®</sup> HDACs Deacetylase fluorometric assay kit, CY-1150), according to the manufacturer's recommendation. Crude nuclear extract from HeLa (10  $\mu$ L) was incubated in buffer for 10 min at 25 °C in the presence of fluoro-substrate (20  $\mu$ M), Lysyl endopeptidase (0.25 mAU/mL) and varying concentrations of inhibitor (from 0.1 to 100  $\mu$ M) in DMSO (10  $\mu$ L), in a total volume of 50  $\mu$ L in 96 well flat-bottomed plates. The fluorescence of each reaction was measured at 37 °C with excitation at 355 nm and emission at 460 nm and data were analyzed as reported above.

### Assays of DHFR Activity

*L. casei* DHFR activity, in the presence and in the absence of inhibitors, has been assayed spectrophotometrically by monitoring the decrease in absorbance at 340 nm due to oxidation of NADPH. All assays were performed at 30 °C in a Shimadzu 2401PC double-beam spectrophotometer. The reaction mixture contained 100  $\mu$ M of dihydro-folic acid, 150  $\mu$ M of NADPH and 2.5  $\mu$ g/mL purified DHFR. The reaction was started by the addition of the enzyme (1-2.5  $\mu$ g) in a final volume of 1.0 mL and read against a blank cuvette containing all components except the enzyme. Synthesized compounds were added in the reaction mixture to final concentrations 0.1-1000  $\mu$ M. For a reference inhibition curve, MTX was added into reaction mixture to final concentrations of 0.001-0.1  $\mu$ M.

### Cell Culture Studies

The lung carcinoma cell line A549 was obtained from American Type Culture Collection. The prostate carcinoma cell line PC3 was a kind gift from Dr. James Norris, Medical University of South Carolina. Cells were maintained in RPMI-1640 supplemented with 10% heat-inactivated fetal bovine serum, 2 mM glutamine and 1 mM sodium pyruvate (complete medium). All cells were grown at 37 °C under humidified air containing 5% CO<sub>2</sub>. Cells were plated in 96-well plates at a density of about 5000 cell/well. Treatment with different concentrations of each inhibitor was performed constantly for 72 h. MTT cell proliferation assay was performed using CellTiter 96 kit (Promega), according to manufacturer's directions.

### Docking Studies

The HDAC8 (PDB code 1T69) and DHFR (PDB code 3DFR) structures taken from the Protein Data Bank were used in this work. After deletion of the correspondent ligands from the active site, hydrogen atoms were added by means of Maestro 7.5 [30,31] using the all-atom model. To assess the reliability and validity of the docking procedure used, the bound ligands were flexibly re-docked into the respective

binding site. The extracted ligands underwent a conformational search of 1000 steps in a water environment (using the generalized-Born/surface-area model) using MacroModel software [31]. The algorithm used was based on the Monte Carlo method with the MMFFs force field and a distance-dependent dielectric constant of 1.0. The ligands were then minimized using the conjugated gradient method until a convergence value of 0.05 kcal/Å mol was reached, using the same force field parameters as those used for the conformational search. The minimized ligands were docked in their corresponding proteins by means of GOLD 3.0.1 [32]. The region of interest used by GOLD was defined in such a manner that it contains the residues which stay within 7 Å from the ligand in the X-ray structures; the zinc ion in HDAC8 was set as trigonal bipyramid atom. The "allow early termination" command was deactivated while the possibility for the ligand to flip ring corners was activated. After setting the remaining Gold parameter with the default values, the ligands were submitted to 200 genetic algorithm runs. Six docking analyses were carried out for HDAC8: in the first three cases, the three fitness functions implemented in GOLD, GoldScore, ChemScore and ASP, were used. In the last three, the formation of hydrogen bonds between the nitrogen atom of His142 and His143 and the ligands was also imposed, and the three fitness functions were used again. In the case of DHFR, only three docking analysis, using the three fitness functions presented in GOLD, were considered. The best docking procedure was then used for further studies. The docking results were evaluated through the comparison of the obtained docked positions of the ligand and the experimental ones. As a measure of docking reliability, the RMSD between the positions of heavy atoms of the ligand in the calculated and the experimental structures was taken into account.

The molecular structures of **1-5** were built, parameterized and energy minimized with Maestro [30]. These ligands were docked into HDAC8 and DHFR active sites using GOLD software and the procedure described above was followed. To perform the docking calculations, the same conditions and parameters which displayed the best prediction of the binding mode of the inhibitors were employed, namely GoldScore scoring function for both enzymes.

### ACKNOWLEDGEMENTS

The authors would like to thank the Portuguese *Fundação para a Ciência e Tecnologia* for financial support. We also thank the Portuguese NMR and MS networks (IST-UTL Center), created by the Portuguese Foundation for Science and Technology (FCT), for providing access to their facilities.

### REFERENCES

- [1] Yoshida, M.; Kijima, M.; Akita, M.; Beppu, T. Potent and specific inhibition of mammalian histone deacetylase both *in vivo* and *in vitro* by trichostatin A. *J. Biol. Chem.*, **1990**, *265*, 17174-17179.
- [2] Korcsmáros, T.; Szalay, M.S.; Böde, C.; Kovács, I.A.; Csermely, P. How to design multi-target drugs. *Expert Opin. Drug Discov.*, **2007**, *2*, 799-808.
- [3] Brown, D.; Superti-Furga, G. Rediscovering the sweet spot in drug discovery. *Drug Discov. Today.*, **2003**, *8*, 1067-1077.

- [4] Bertino, J.R. Karnofsky memorial lecture. Ode to methotrexate. *J. Clin. Oncol.*, **1993**, *11*, 5–14.
- [5] Smorenburg, C.H.; Spareboom, A.; Bontenjal, M.; Verweij, J. Combination chemotherapy of the taxanes and antimetabolites: its use and limitations. *Eur. J. Cancer*, **2001**, *37*, 2310–2323.
- [6] Schnell, J.R.; Dyson, H.J.; Wright, P.E. Structure, dynamics, and catalytic function of Dihydrofolate Reductase. *Annu. Rev. Biophys. Biomol. Struct.*, **2004**, *33*, 119–140.
- [7] Hildmann, C.; Riestler, D.; Schwienhorst, A. Histone deacetylases: an important class of cellular regulators with a variety of functions. *Appl. Microbiol. Biotechnol.*, **2007**, *75*, 487–497.
- [8] Takimoto, C.H. New Antifolates: Pharmacology and Clinical Applications. *The Oncologist*, **1996**, *1*, 68–81.
- [9] Finn, P.W. *Histone Deacetylase Inhibitors*, in *Drug Design of Zinc-Enzyme Inhibitors*; Supuran, C.T.; Winum, J.-Y. Ed.; John Wiley & Sons Inc, **2009**, pp. 859–879.
- [10] Marks, P.A.; Xu, W.-S. Histone deacetylase inhibitors: Potential in cancer therapy. *J. Cell. Biochem.*, **2009**, *107*, 600–608.
- [11] Buchwald, M.; Krämer, O.H.; Heinzl, T. HDACi – Targets beyond chromatin. *Cancer Lett.*, **2009**, *280*, 160–167.
- [12] Bora-Tatar, G.; Dayanç-erden, D.; Demir, A.S.; Dalkara, S.; Yeleği, K.; Erdem-Yurter, H. Molecular modifications on carboxylic acid derivatives as potent histone deacetylase inhibitors: Activity and docking studies. *Bioorg. Med. Chem.*, **2009**, *17*, 5219–5228.
- [13] Grolla, A.A.; Podestà, V.; Chini, M.G.; Di Micco, S.; Vallario, A.; Genezzani, A.A.; Canonico, P.L.; Bifulco, G.; Tron, G.C.; Sorba, G.; Pirali, T. Synthesis, Biological Evaluation, and Molecular Docking of Ugi Products Containing a Zinc-Chelating Moiety as Novel Inhibitors of Histone Deacetylases. *J. Med. Chem.*, **2009**, *52*, 2776–2785.
- [14] Marks, P.A. Discovery and development of SAHA as an anticancer agent. *Oncogene*, **2007**, *26*, 1351–1356.
- [15] Zimmermann, G.R.; Lehar, J.; Keith, C.T. Multi-target therapeutics: when the whole is greater than the sum of the parts. *Drug Discov. Today*, **2007**, *12*, 34–42.
- [16] Tumber, A.; Collins, L.S.; Petersen, K.D.; Thougard, A.; Christiansen, S.J.; Dejligbjerg, M.; Jensen, P.B.; Sehested, M.; Ritchie, J.W.A. The histone deacetylase inhibitor PDX101 synergises with 5-fluorouracil to inhibit colon cancer cell growth *in vitro* and *in vivo*. *Cancer Chemother. Pharmacol.*, **2007**, *60*, 275–283.
- [17] Bots, M.; Johnstone, R.W. Rational Combinations Using HDAC Inhibitors. *Clin. Cancer Res.*, **2009**, *15*, 3970–3977.
- [18] Mukherjee, P.; Pradhan, A.; Shah, F.; Tekwani, B.L.; Avery, M.A. Structural insights into the *Plasmodium falciparum* histone deacetylase 1 (PFHDAC-1): A novel target for the development of anti-malarial therapy. *Bioorg. Med. Chem.*, **2008**, *16*, 5254–5365.
- [19] Richon, V.M.; Garcia-Vargas, J.; Hardwick, J. S. Development of vorinostat: Current applications and future perspectives for cancer therapy. *Cancer Lett.*, **2009**, *280*, 201–210.
- [20] Marques, S.M.; Nuti, E.; Rossello, A.; Supuran, C.T.; Tuccinardi, T.; Martinelli, A.; Santos, M.A. Dual inhibitors of matrix metalloproteinases and carbonic anhydrases: iminodiacetyl-based hydroxamate–benzenesulfonamide conjugates. *J. Med. Chem.*, **2008**, *51*, 7968–7979.
- [21] Santos, M.A.; Enyedy, E.A.; Rossello, A.; Carelli, P.; Krupenko, N.I.; Krupenko, S.A. Methotrexate  $\gamma$ -hydroxamate derivatives as potential dual target antitumor drugs. *Bioorg. Med. Chem.*, **2007**, *15*, 1266–1274.
- [22] Marques, S.M.; Enyedy, E.A.; Supuran, C.T.; Krupenko, N.I.; Krupenko, S.A.; Santos, M.A. Pteridine-sulfonamide conjugates as dual inhibitors of carbonic anhydrases and dihydrofolate reductase with potential antitumor activity. *Bioorg. Med. Chem.*, **2010**, *18*, 5081–5089.
- [23] Low, P.S.; Kularatne, S.A. Folate-targeted therapeutic and imaging agents for cancer. *Curr. Opin. Chem. Biol.*, **2009**, *13*, 256–262.
- [24] Reynolds, R.C.; Campbell, S.R.; Fairchild, R.G.; Kisliuk, R.L.; Micca, P.L.; Queener, S.F.; Riordan, J.M.; Sedwick, W.D.; Waud, W.R.; Leung, A.K.; Dixon, R.W.; Suling, W.J.; Borhani, D.W. Novel boron-containing, non-classical antifolates: synthesis and preliminary biological and structural evaluation. *J. Med. Chem.*, **2007**, *50*, 3283–3289.
- [25] Finnin, M.S.; Donigian, J.R.; Cohen, A.; Richon, V.M.; Rifkind, R.A.; Marks, P.A.; Breslow, R.; Pavletich, N.P. Structures of a histone deacetylase homologue bound to the TSA and SAHA inhibitors. *Nature*, **1999**, *401*, 188–193.
- [26] Vannini, A.; Volpari, C.; Gallinari, P.; Jones, P.; Mattu, M.; Carfi, A.; De Francesco, R.; Steinkühler, C.; Di Marco, S. Substrate binding to histone deacetylases as shown by the crystal structure of the HDAC8-substrate complex. *EMBO Reports*, **2007**, *8*, 879–884.
- [27] Armarego, W.; Perring, D. *Purification of Laboratory Chemicals*. Butterworth-Heinemann Press, **1999**.
- [28] SoftMax Pro 4.7.1 by Molecular Device.
- [29] GraFit version 4 by Erithecus Software.
- [30] Maestro, version 7.5; Schrödinger Inc.: Portland, OR, **2005**.
- [31] MacroModel, version 8.5; Schrödinger Inc.: Portland, OR, **1999**.
- [32] Jones, G.; Willett, P.; Glen, R.C.; Leach, A.R.; Taylor, R. Development and validation of a genetic algorithm for flexible docking. *J. Mol. Biol.*, **1997**, *267*, 727–748.